

Tin removal from extreme ultraviolet collector optics by inductively coupled plasma reactive ion etching

H. Shin,^{a)} S. N. Srivastava, and D. N. Ruzic^{b)}

Center for Plasma Material Interactions, University of Illinois at Urbana-Champaign, Urbana, Illinois 61801

(Received 12 October 2007; accepted 25 February 2008; published 4 April 2008)

Tin (Sn) has the advantage of delivering higher conversion efficiency compared to other fuel materials (e.g., Xe or Li) in an extreme ultraviolet (EUV) source, a necessary component for the leading next generation lithography. However, the use of a condensable fuel in a lithography system leads to some additional challenges for maintaining a satisfactory lifetime of the collector optics. A critical issue leading to decreased mirror lifetime is the buildup of debris on the surface of the primary mirror that comes from the use of Sn in either gas discharge produced plasma (GDPP) or laser produced plasma (LPP). This leads to a decreased reflectivity from the added material thickness and increased surface roughness that contributes to scattering. Inductively coupled plasma reactive ion etching with halide ions is one potential solution to this problem. This article presents results for etch rate and selectivity of Sn over SiO₂ and Ru. The Sn etch rate in a chlorine plasma is found to be much higher (of the order of hundreds of nm/min) than the etch rate of other materials. A thermally evaporated Sn on Ru sample was prepared and cleaned using an inductively coupled plasma etching method. Cleaning was confirmed using several material characterization techniques. Furthermore, a collector mock-up shell was then constructed and etching was performed on Sn samples prepared in a Sn EUV source using an optimized etching recipe. The sample surface before and after cleaning was analyzed by atomic force microscopy, x-ray photoelectron spectroscopy, and Auger electron spectroscopy. The results show the dependence of etch rate on the location of Sn samples placed on the collector mock-up shell. © 2008 American Vacuum Society. [DOI: 10.1116/1.2899332]

I. INTRODUCTION

In the microelectronics industry, lithography currently limits the minimum feature size due to the wavelength of the light source used.¹ Extreme ultraviolet (EUV) lithography can produce smaller and faster transistors because of its short wavelength (13.5 nm) and, therefore, has been chosen by the semiconductor industry as the main contender for future chip manufacturing at the 22 nm node and beyond.² Lenses have always been used to collect light in lithography processes, but in the case of EUV lithography, mirrors must be used (instead of lenses) to focus light onto a mask since no materials are transparent at 13.5 nm. The reflectivity of the mirrors strongly affects the pattern quality and reflected EUV light flux. The collector optics—the mirrors nearest to the source—are particularly susceptible to reflectivity degradation due to harsh plasma debris. Reflectivity degradation would cause frequent replacement of mirrors which is economically not feasible.

Of various causes for this reflectivity loss, the energetic ion debris from the plasma source is the most important since it erodes the material and roughens the surface, contributing to scattering.³ Debris buildup is an additional problem when Sn is used as a main fuel for EUV light sources in either gas discharge produced plasma (GDPP) or laser pro-

duced plasma (LPP) because of its condensable nature ($T_b = 2270$ °C).⁴ The use of Sn is preferable because it has relatively higher conversion efficiency (~2%) than other EUV fuel materials such as xenon (Xe) or lithium (Li).⁵ With a solid Sn target in LPP, an even higher conversion efficiency (3%) was reported.⁶ To increase the lifetime of collector mirrors, debris mitigation techniques^{7,8} and cleaning methods need to be investigated together. Debris mitigation techniques are being developed to prevent damage and, in turn, keep the reflected EUV output maximum, whereas cleaning methods are essential to recover the reflectivity in the case of abnormal events. Although mitigation techniques slow down Sn debris deposition, they cannot eliminate the debris buildup problem. For example, Sn deposition rates in an EUV system were reported to be as much as 3.9×10^{-4} nm/pulse without any mitigation techniques and 3.2×10^{-6} nm/pulse with a mitigation technique.⁹ Harilal *et al.*¹⁰ summarized and listed several different concepts to mitigate ion debris, such as using tape targets, ambient gas for moderating the species, foil trap, cavity confinement, electrostatic repeller fields, magnetic fields, and mass limited targets. An atomic hydrogen cleaning method for removing Sn as well as C showed the feasibility of cleaning EUV mirrors with a removal rate higher than 200 nm/h.^{11,12}

The cleaning methods described above have too low removal rates and exhibit insufficient cleaning for many applications. If inductively coupled plasma reactive ion etching (ICP-RIE) processes are developed for cleaning, the ion en-

^{a)} Author to whom correspondence should be addressed; electronic mail: shin5@uiuc.edu

^{b)} Electronic mail: druzic@uiuc.edu

hanced surface reactions could be used for more effective and faster Sn removal. If a plasma can selectively etch debris on mirrors under certain conditions, even *in situ* cleaning could be possible and save significant time and cost. This work on Sn cleaning shows that etching with Ar/Cl₂ plasma can remove Sn significantly fast (several hundreds of nm/min). Therefore, it may be possible to conduct ICP-RIE Sn cleaning without severe damage to mirror surfaces if the mirror surfaces are resistant to etching.

In the current investigation, the etch rate of Sn with an Ar/Cl₂ plasma has been measured for the first time by changing the substrate rf bias as the primary independent variable. For most Mo/Si multilayer EUV mirrors (used for normal incidence), Si or Ru is used as a protective capping layer.¹³ For a Si capping layer, there always exists a thin native oxide layer on the surface (SiO₂). Thus, for the selectivity study, Ru, Si, and SiO₂ were chosen for the etch rate comparison with Sn. Moreover, Ru is also widely used for coating grazing incidence mirrors due to its high reflectivity for EUV and high oxidation resistance. Therefore, the selectivity results between Sn and Ru would be applicable for ICP-RIE cleaning of both normal incidence mirrors and grazing incidence mirrors. To study Sn cleaning beyond an etch rate selectivity measurement, Sn was deposited on Ru samples by thermal evaporation and plasma cleaning was performed. Furthermore, to simulate the mirror geometry, a mirror shell mock-up was constructed out of stainless steel shim stock and mirror samples exposed to a Sn EUV source were placed on the shells. Pre- and postcleaning sample surfaces were characterized by a variety of surface analysis techniques such as x-ray photoelectron spectroscopy (XPS), Auger electron spectroscopy (AES), and atomic force microscopy (AFM) to study the success and side effects of the cleaning process.

II. EXPERIMENT

The etching chamber at the Center for Plasma Material Interactions is equipped with a stainless steel two-turn internal coil for the inductively coupled plasma source. It also includes a MKS mass flow controller connected to a Java computer program controller, 1200 l/s Ar speed Helix cryopump, 500 l/s Ar speed Pfeiffer turbo pump, Dryvac 100P dry pump for handling corrosive gases, an ion gauge, convector gauges, a baratron gauge, and an exhaust handling system for chlorine gas. The system uses two 13.56 MHz rf power supplies—Balzers RFS 301 and ENI ACG-3DC. The RFS 301 is used for the ICP coil plasma source and the ENI ACG-3DC is used for the chuck rf bias. Both rf power supplies are connected to rf matching networks to minimize reflected power. To study the cleaning of Sn on collector mock-up shells, however, the rf power supply to the chuck was replaced by a dc power supply for easier biasing control.

The use of an internal ICP coil in the present experiment caused the unwanted sputtering of coil material, which redeposited on the chamber wall and samples. Therefore, additional care was taken to minimize the sputtered materials from the stainless steel antenna coil. By using glass cloth

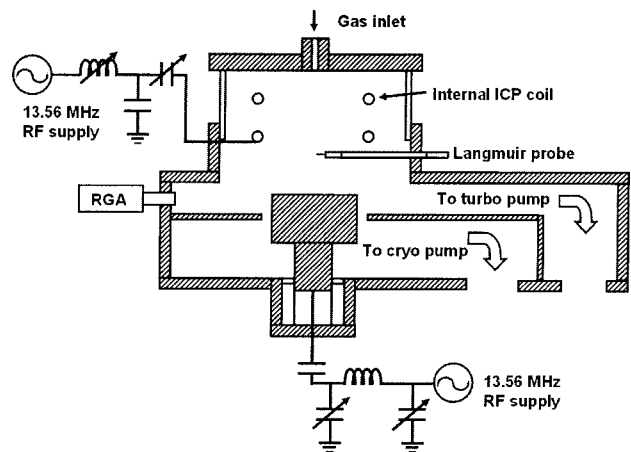


FIG. 1. Schematic of the ICP etching apparatus.

tape to wrap the coil, the stainless steel coil was prevented from sputtering and was also electrically isolated from the plasma. The glass cloth materials can still be sputtered by the potential difference between the plasma and the coil. However, the insulated coil lowers the plasma potential so as to reduce the sputtering.¹⁴ The higher electron density in the insulated coil system is another reason to use the glass cloth tape for our internal coil.¹⁴ Figure 1 shows the simplified schematic of the ICP-RIE chamber. The chamber contains separate gas feedthroughs which allow more controlled flow of gases of desired inputs. The electron density of the Ar/Cl₂ plasma is $(2.9 \pm 0.4) \times 10^{11} \text{ cm}^{-3}$, determined using a rf compensated Langmuir probe. The electron temperature T_e measured in the same manner is around 3 eV.¹⁵ Since the system in the present experiment was not equipped with a load-lock system to minimize water adsorption after each run, a residual gas analyzer (RGA) was utilized for monitoring water vapor pressure before each experimental run. The chamber was baked out using halogen lights, and the water vapor pressure could be minimized down to 30% of total pressure when analyzed with a RGA. The total base pressure of the system was 2.9×10^{-7} Torr after being baked out.

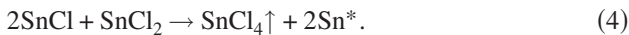
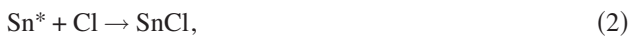
The etch rates of Sn, Si, Ru, and SiO₂ were first measured in this study. For the etch rate measurement, the samples were half covered with a piece of SiO₂ wafer and were processed for certain time. A stylus-type profilometer was used to measure the depth change after the etching was performed. Total etched depth was divided by the processing time to get the etch rate of each material. Initial experiments were performed with 1 μm Sn on a Si₃N₄ substrate, deposited by sputtering. Ru samples were prepared by ion beam sputtering on a Si substrate. It is realized that Sn is etched extremely fast and even a small processing time (~2 min) is enough to remove a 1 μm Sn layer. To do the profilometry measurements, the processing time was reduced to 1 min so that a reasonable depth change could be seen without over etching. In the cases of Si, Ru, and SiO₂, the depth change could not be measured if processed for 1 min. The etch depth in these cases is less than 10 nm under the investigated conditions,

which is the resolution of the profilometer. To be able to measure the depth change, all other samples (except Sn) were processed for 10 min.

In this study, a couple of more experiments followed the etch rate measurement to investigate Sn cleaning with this ICP-RIE method. For those experiments, samples were accordingly prepared and more details of the samples are described with results.

III. RESULTS AND DISCUSSION

This article presents the result of Sn cleaning using an Ar/Cl₂ plasma. When using the Ar/Cl₂ plasma, it is important to understand the surface kinetics of Sn etching, as described simply in Eqs. (1)–(4),



Dangling bonds are formed when ions from the plasma impinge on to the Sn surface and create active sites (Sn*) for physisorption or chemisorption of Cl atoms (etchants). According to the Langmuir–Hinshelwood mechanism,¹⁶ the adsorbed molecules such as SnCl and SnCl₂ react with each other on the surface to make tin tetrachloride (SnCl₄), which is a volatile product. Incident ions will enhance the reaction in Eq. (4) by transferring energy to the surface. The importance of ions in the etching process is realized as they create more active sites on the surface and enhance the reaction rate.

It was mentioned that a RGA was used to monitor the water vapor pressure level in the system for proper etching. During the etch rate measurement, it was found that the etch rate was not easily reproducible since water severely interferes with Sn etching. It appears that water molecules remaining in the chamber possibly react with etchant to form hydrogen chloride (HCl) and deplete etchant density. A more likely reason could be that the Sn surface is rapidly passivated by an oxide layer when much O₂ and H₂O are present in the plasma, as is known in Al etching.¹⁷ The etch rate decrease due to etchant depletion or Sn surface passivation is shown in Fig. 2. When the water vapor pressure is higher than 1×10^{-5} Torr, Sn does not etch at all under the conditions of 20 mTorr processing pressure, 5 SCCM Ar/25 SCCM Cl₂ gas mixture (SCCM denotes cubic centimeter per minute at STP), 500 W ICP power and –77 V bias. With lower water pressure, Sn starts to etch, but the etch rates at 2.6×10^{-7} and at 7.0×10^{-8} Torr are considerably different. This implies the significance of water vapor pressure for Sn etching with chlorine plasma.

The gas mixture was optimized for the best etching. At a fixed pressure and total flow rate, the amount of Ar was varied to observe the effect on etching. Figure 3 shows the effect of changing the gas mixture ratio on the etch rate of Sn

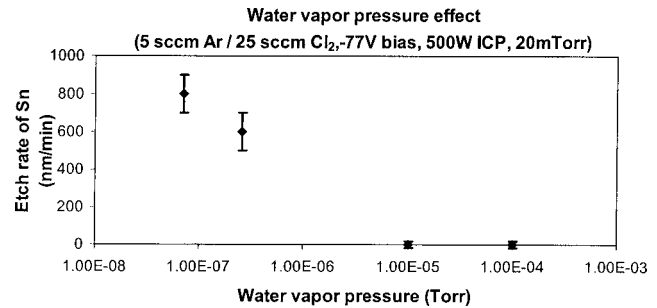


FIG. 2. Variation of etch rate with water vapor pressure at 5 SCCM Ar/25 SCCM Cl₂, –77 V bias, 500 W ICP power, and 20 mTorr processing pressure. Low water vapor pressure enhances the etching. Water vapor pressure is in a log scale.

samples. Other than the gas mixture ratio, all the conditions are fixed: –77 V rf bias, 500 W ICP power, 20 mTorr processing pressure, and 30 SCCM total flow rate. With no Cl₂, etching results are purely from Ar ion sputtering due to the absence of etchant (Cl atoms). This physical etching produces the lowest etch rate at –77 V bias. The Sn etch rate increases as the Cl₂ flow rate increases from 0 to 25 SCCM (increased etchant). It was noticed that the small addition of 5 SCCM Ar to 25 SCCM Cl₂ greatly enhanced the etch rate and produced a greater rate than when just using 30 SCCM of Cl₂. This shows that the presence of Ar ions enhances reactive etching by creating more active sites as previously described in Eq. (1) as well as hitting the surface and transferring energy to the surface. Although there are positive chlorine ions (Cl⁺, Cl₂⁺) to enhance the surface reactions, the effects are less compared to Ar ions because of the smaller fraction of positive chlorine ions in 30 SCCM Cl₂ plasma than Ar ions in 5 SCCM Ar plasma. The etch rates rather decrease with Ar flow rates greater than 5 SCCM. The reason why the etch rate decreases with higher fraction of Ar in the gas is due to the decrease of the etchant. A combination of 10 SCCM Ar and 20 SCCM Cl₂ was used for the etch rate study shown in Fig. 4. The optimal mixture ratio (5 SCCM Ar and 25 SCCM Cl₂) was used for the rest of this study.

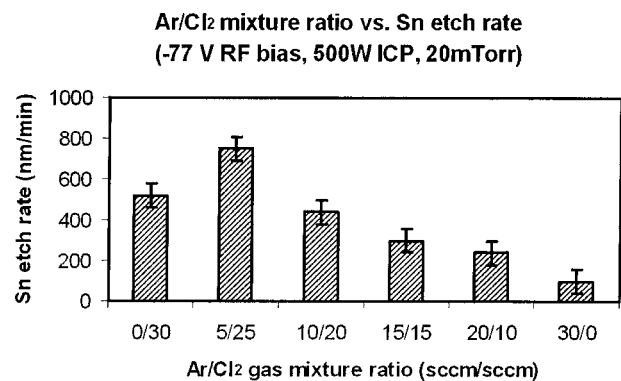


FIG. 3. Variation of etch rate as a function of Ar/Cl₂ gas mixture ratio. Optimized ratio is found as 5 SCCM Ar/25 SCCM Cl₂ at –77 V bias, 500 W ICP power, 1.5×10^{-7} Torr water vapor pressure and 20 mTorr processing pressure.

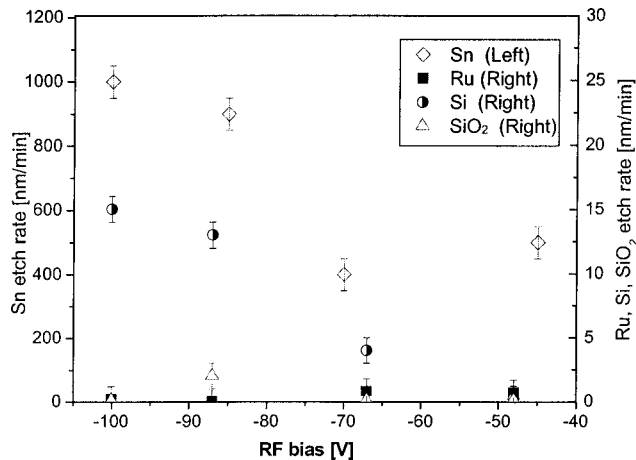


FIG. 4. Etch rates of Sn, Si, Ru, and SiO₂ as a function of rf bias. Sn samples are processed for 1 min, whereas Ru, Si, and SiO₂ are processed for 10 min. Sn etch rate is on the left y axis. The etch rate of Sn is orders of magnitude higher than for the other materials. For this experiment, a combination of 10 SCCM Ar and 20 SCCM Cl₂ was used.

Figure 4 shows the etch rates of Sn, Si, Ru, and SiO₂ using Ar/Cl₂ plasma. The etch rate in nm/min is plotted against rf bias voltage in volts with the following experimental constants: 500 W source power, 10 SCCM/20 SCCM Ar/Cl₂ flow rates, $\sim 1.5 \times 10^{-7}$ Torr water vapor pressure, and 20 mTorr total processing pressure. rf bias is the self-developed dc negative voltage due to the different mobility of electrons and ions in an asymmetric geometry. It is a complicated function of reactor geometry, the blocking capacitor value, matching network parameters, and ion bombardment energy.¹⁸ However, rf bias is a good indicator for the ion bombardment energy. Plasma power directly affects the density of the plasma and, accordingly, high power will increase etch rate. However, for stable operation, the power was fixed at 500 W for the etch rate measurement. The etch rate of Sn is plotted on the left y axis, whereas the etch rates of other materials are plotted on the right y axis. Interesting information can be derived from this figure. First of all, the etch rate is a strong function of the bias voltage. The rate goes higher with increasing bias voltage. When using a higher bias (~ -100 V), 1 μm -thick Sn seems to be completely etched. This trend shows that the kinetic energy of ions enhances the etching process. The Si etch rate data show the similar trend with Sn but the rates are two orders of magnitude lower. It is worthwhile to note that the SiO₂ and Ru etch rates are extremely low under the same experimental conditions.

Secondly, the comparison of the Sn etch rate with other materials (Si, SiO₂, and Ru) provides the motivation to continue this investigation toward developing this technology for *in situ* cleaning in EUV lithography. It can be seen that right y-axis scale is of several orders of magnitude less than that of the left y-axis scale. Sn etch rate, which is plotted on the left side, is much higher compared to those of the other materials. This means that Sn can be etched by this method without damaging the Ru layer or SiO₂ layer on top of the collector optics. For a Si-capped mirror, however, a native

oxide is very thin (~ 1 nm) and may be etched faster than a bulk sample used for this study. Therefore, the small erosion of SiO₂ could be unfavorable for ICP-RIE cleaning method for the Si-capped mirrors. Nevertheless, the reluctance of Ru for Ar/Cl₂ etching under the conditions investigated is a promising result for the Ru-capped multilayer mirrors for LPP or Ru-coated grazing incidence mirrors for GDPP. The etch rate measurement results imply that this ICP-RIE cleaning method is more suitable for Ru surface mirrors. So, the rest of the experiment was focused on Ru surface mirrors. The etch rate selectivity of Sn over Ru varies depending on the rf bias, from around 500 (at -45 V) to 1000 (at -90 V). There is much uncertainty in calculating the value of selectivity due to reading errors of etch rate measurements with a profilometer. Nonetheless, such a huge selectivity over a wide range of bias is very promising for cleaning Sn from mirror surfaces. Sn is etched with a significantly faster rate even at low bias, where the ion energies are small so as not to damage the underlying surface after complete removal of Sn. Although serious physical sputtering of Ru was not observed in this experiment, there is a concern that ions with energy much higher than the sputtering threshold voltage could potentially damage the surface.

As seen in the etch rate results, this plasma etching method can clean Sn very fast. This fact is very favorable for the Sn source system. Based on the experiment of Teramoto *et al.*⁹ for the Sn buildup rate, a simple estimation of cleaning cycles can be calculated. In their DPP EUV system, Sn deposits on the mirrors with a rate of 3.9×10^{-6} nm/pulse with debris mitigation techniques and, for example, 1000 s operation with a pulse rate of 1 kHz will deposit about 4 nm Sn on the mirror surface. The 4 nm Sn on the Ru surface grazing incidence (10°) mirror will degrade the EUV reflectivity as much as 30%.¹⁹ Since the surface roughness also affects the reflectivity, the real reflectivity loss from the source can be worse. However, plasma cleaning can remove Sn in a few seconds so that it does not cause any serious tool down time. Also, it is possible to clean *in situ* without breaking the vacuum of the source chamber.

As this technique could clean Sn debris buildup from the mirrors effectively fast, several other experiments were performed to study Sn cleaning in more detail. To start with, the samples for cleaning were prepared by depositing about 100 nm Sn on a Ru surface in a bell-jar thermal evaporator. To minimize oxygen mixed into deposited Sn layer, Sn was evaporated first without mounting the Ru sample, to coat the chamber wall. Samples were then processed at the lowest possible pressure achieved in the system. Sn samples deposited on Ru were cleaned by an optimized etching recipe, and then the surface was scanned by AES to verify the Sn removal from the Ru surface. AES was also used to investigate the surface damages such as ion implantation from plasma into the underlying layers.

Figures 5(a) and 5(b) show the AES depth profiles of 100-nm-thick Sn on Ru samples before and after cleaning, respectively, at the optimized experimental conditions. The processing time was 3 min as this was long enough to re-

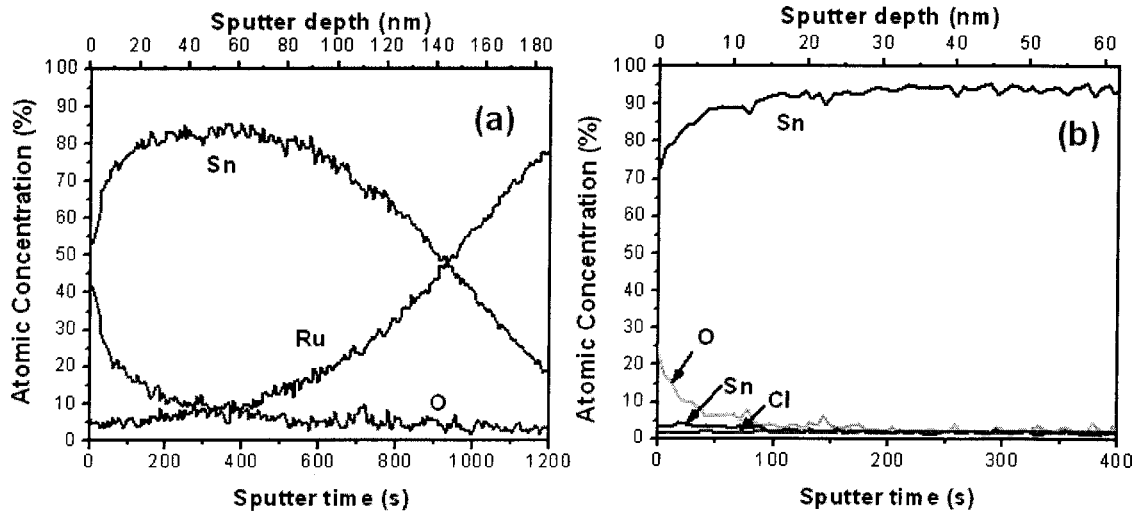


FIG. 5. AES analysis of pre- and postprocessed samples. These are 100 nm of Sn deposited on a Ru substrate by thermal evaporation. Cleaning was performed for 3 min. (a) Before cleaning: Sn can be seen on the surface. (b) After cleaning: Sn is completely removed.

move the Sn completely from the Ru surface and to investigate if the surface gets damaged by plasma etching. In Fig. 5(a), despite the oxygen control during deposition, a small amount ($\sim 5\%$) of oxygen was still detected on the deposited Sn layer. The reason why the curves gradually change is mainly explained by two factors: (1) the interface between Ru and Sn is not clear at all due to their diffusion to each other layer and (2) Ar ions used for sputtering for AES may push the element on the surface into the underlying layer. This will make us see Sn in a deeper region than its real thickness. A thickness of 100 nm is an approximation and there is some error when converting the sputter time to sputter depth since sputtering yield is different for the different layers. The Sn has been found to be completely removed from the Ru after 3 min cleaning with Ar/Cl₂ plasma, as shown in Fig. 5(b). Moreover, there was no evidence of ion implantation in the Ru layer either in the AES analysis. If ions from the plasma are implanted into the Ru layer, more Cl should be seen in the AES result especially on the top surface region than that seen in Fig. 5(b). This AES result shows the complete removal of Sn as well as no damage to the mirror surface for the chosen cleaning cycle.

It is of more interest to see if the developed cleaning technique would actually work in the complex geometry of the EUV collector mirror shells. To aid this investigation, the collector mock-up shells were constructed and placed in a nested configuration to mimic the geometry of the real collector optics, as shown in Fig. 6. A real EUV collector for grazing incident mirrors has multiple shells to increase light collection. Stainless shim stock was used here to make the cylindrical collector mirror mock-ups. The rf coils for the ICP plasma were placed over the mock-up shells, and a 10 mm spacing was left at the bottom of the chuck which provides a path for the gas flow. This would enhance plasma penetration and the removal of etching products. For this study, smooth Ru samples on the nickel substrate were provided by a supplier. The Ru samples were exposed to the Sn

EUV source, and a thin layer of Sn was deposited on the surface. A quartz crystal microbalance was used to measure the Sn deposition thickness, which was about 3 nm. These Sn contaminated Ru samples were then placed at three different positions (top, middle, and bottom) on a cylindrical mock-up shell. The source power in this case was increased to 700 W, assuming that the plasma loss in collector mock-up shells will be more. The mock-up shells were biased at -100 V by dc voltage supply. Two different sets of measurements were performed, and the effect of processing time on final etching was investigated. All the other experimental conditions were the same in both measurements.

The first set of samples was cleaned for 1 min. Post-cleaned samples were characterized using several material characterization techniques such as XPS, AES, and AFM. Figure 7 shows the XPS results of the first set of samples from the mirror mock-up simulations. All three postpro-

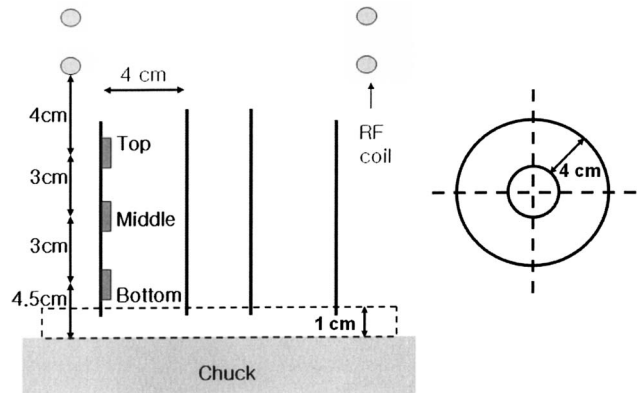


FIG. 6. Schematic of collector mirror mock-up shells. Three samples are positioned at different locations (top, middle, and bottom). The right figure shows the top down view of the nested two-shell collector mirror mock-up. Note that there is a 1 cm spacer for a better gas flow between the mock-up and the chuck.

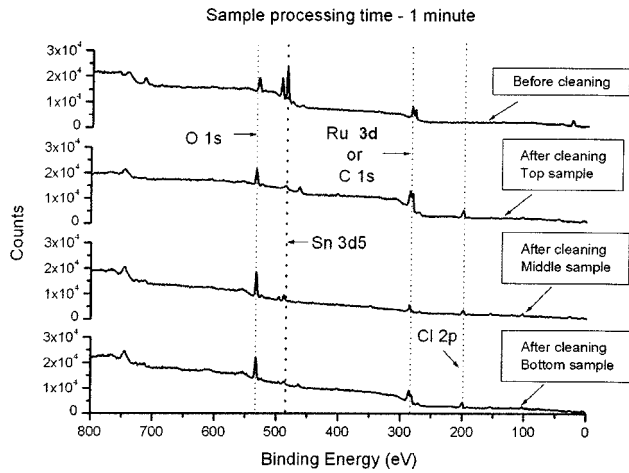


Fig. 7. XPS analysis of pre- and postprocessed samples. These are 3 nm of Sn deposited on a Ru substrate in a real Sn EUV source. Cleaning was performed for 1 min. Sn peak can be seen very clearly on the sample before cleaning, whereas a considerable reduction in this peak is noticed after cleaning the Sn from samples at different locations on the mock-up shells.

cessed samples show a significant reduction in the Sn peak compared to the preprocessed samples. This means that Sn on the Ru surface has been mostly removed by the 1 min Ar/Cl₂ plasma etching. A very weak Sn signal is still seen in the XPS results. This implies that some Sn residue remains on the surface after cleaning. Cl was also detected on the surface for all three samples. This Cl peak could be from ruthenium chloride (RuCl₃) or adsorbed Cl atoms which are not involved in the formation of the volatile SnCl₄. The high resolution scan over Ru's binding energy range (Fig. 8) clearly shows the presence of RuCl₃ after cleaning.

Although XPS provides much information about the surface after cleaning, AES was also used to confirm the XPS result and to study the depth profile. While 3 keV Ar ion beam sputters the surface at a rate of 2.9 Å/min, a depth profile of each element can be collected. Before collecting data, the surface was cleaned by ion sputtering for 0.2 min for this AES scan. Figure 9 shows the AES results of the first set of samples from the mirror mock-up simulations. It is

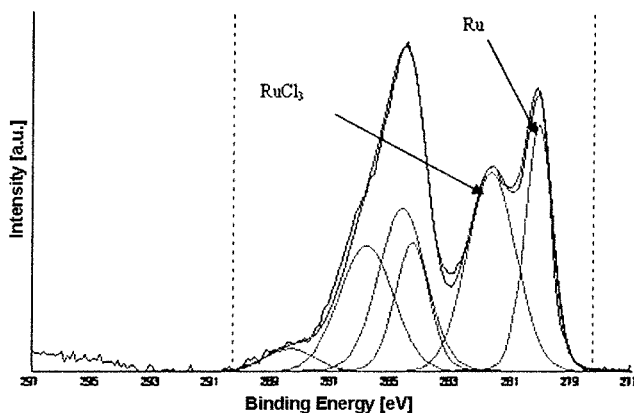


Fig. 8. High resolution XPS scan of postprocessed sample (top sample) shows the presence of RuCl₃. All the samples show a similar trend.

revealed that there is oxide formation as much as Sn in the Sn layer before cleaning [Fig. 9(a)]. This oxide could originate from the EUV source chamber or from air after unloading samples from the EUV exposure chamber. In the depth profile measurement of the preprocessed sample, Sn is seen in the Ru layer because the Ar ion beams used in this measurement (for sputtering) probably pushed it in the surface material while sputtering the surface. Energetic Sn ion implantation during EUV exposure might be considered as well, but after cleaning, the results do not show a significant amount of Sn in the Ru layer. There must be Sn in the Ru layer if it existed before cleaning. Using AES results, it was confirmed again that Sn has been removed from the surface at all three locations by the 1 min cleaning process. The Cl signal is ignorable in all three samples [Figs. 9(b)–9(d)].

To study the surface roughness, pre- and postprocessed samples were characterized using AFM. Figure 10 shows the captured AFM images of all the samples in the first set of measurements. The polishing scratches are clearly seen which account for relatively high rms roughness. It should be noted that these scratch marks are not due to the cleaning but were present on the original samples before cleaning. These polishing scratches are from the Ru surface, which was provided by a supplier. The middle sample [Fig. 10(b)] does not have those scratches, although it was from the same supplier. Measured rms roughnesses for preprocessed samples are 6.7, 3.2, and 5.9 nm for the top, middle, and bottom samples, respectively. Postprocessed rms roughnesses for these samples are 6.5, 1.2, and 4.8 nm respectively. Table I summarizes the rms roughness data. Due to the absence of scratches of the middle sample, rms roughness of the middle sample is significantly lower than the others. However it is important to compare the roughness before and after cleaning for this study. It is promising that surface roughness is somewhat reduced after cleaning.

The results presented so far show that considerable cleaning can be achieved using the ICP-RIE method in a complex geometry, and that this technique can be considered for integrating into the source collector module for *in situ* cleaning. Nevertheless, in high volume manufacturing (HVM), the processing time is critical. Although 1 min cleaning is short, an even shorter processing time could be more advantageous in HVM applications. To address this issue, three more samples were cleaned using ICP-RIE for only 20 s to see the effect of processing time.

The second set of samples was processed in the same manner but for only 20 s. Figure 11 shows the XPS results of the second set of samples from the mirror mock-up simulations. Even with a 20 s cleaning, Sn on the top and middle sample is mostly removed. With a negative bias as high as –100 V, removing a thin Sn from the sidewall for a short time seems to work, even though the sample was placed between two conducting shells. However, the bottom sample still has a considerable amount of Sn left on the surface. One other noticeable result in the XPS data is that oxidation on the surface is less than that of the first set of samples, which were processed for 1 min.

Sample processing time – 1 minute

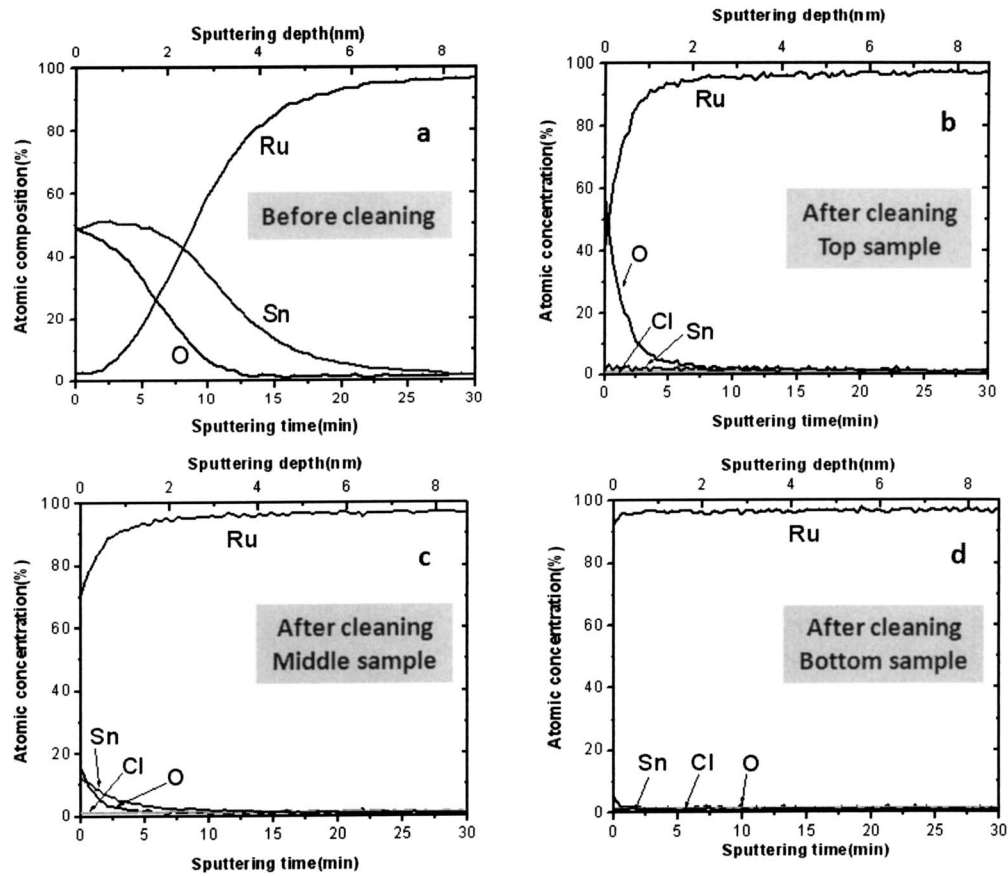


FIG. 9. AES analysis of pre- and postprocessed samples. These are 3 nm of Sn deposited on a Ru substrate in a real Sn EUV source. Cleaning was performed for 1 min. (a) Preprocessed sample, (b) postprocessed top sample, (c) postprocessed middle sample, and (d) postprocessed bottom sample. Sn is considerably removed from all the three postprocessed samples.

Sample processing time – 1 minute

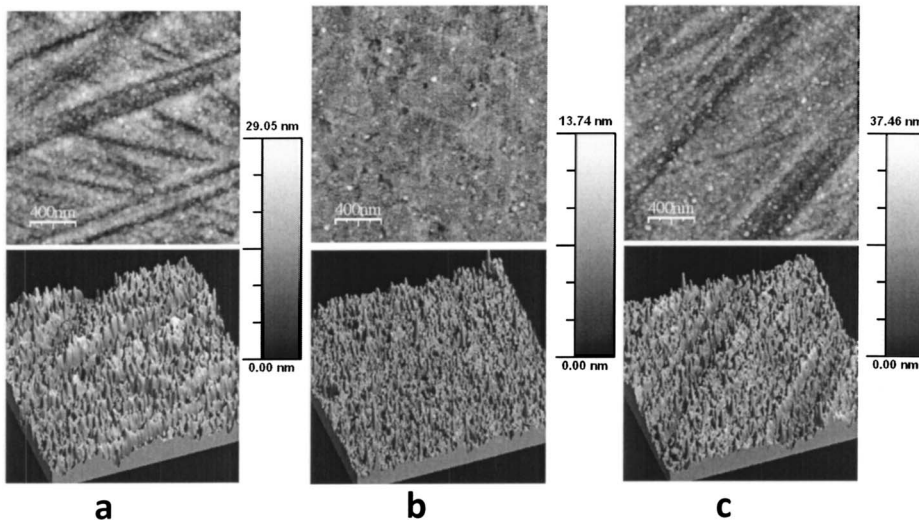


FIG. 10. AFM analysis of postprocessed samples. These are 3 nm of Sn deposited on a Ru substrate in a real Sn EUV source. Cleaning was performed for 1 min. (a) Postprocessed top sample, (b) postprocessed middle sample, and (c) postprocessed bottom sample.

TABLE I. AFM results of before-cleaning and after-cleaning samples after 1 min of processing time. The root mean square roughness (R_{rms}) and the maximum height (H_{max}) values for three postprocessed samples are shown in the table.

Position	Before cleaning		After cleaning	
	R_{rms} (nm)	H_{max} (nm)	R_{rms} (nm)	H_{max} (nm)
Top	6.7	55.3	6.5	93.7
Middle	3.2	38.6	1.2	14.4
Bottom	5.9	51.5	4.8	47.8

Figure 12 shows the AES results for the second set of samples from the mirror mock-up simulations. This confirms the XPS observation. It can be seen that there is less oxidation in this process [Figs. 12(b) and 12(c)] and that the Sn is not completely removed from the bottom sample as seen in XPS results [Fig. 12(d)]. The bottom sample's depth profile shows much oxygen (40%). This oxygen is not from the new oxidation induced by cleaning but from the original sample because a considerable amount of Sn (~40%) still remains together with oxygen. The similarity of the profiles in Fig. 12(a) deeper than 1 nm and Fig. 12(d) supports this explanation.

Figure 13 shows the AFM images of the second set of samples after cleaning in the mirror mock-up simulations.

The measured rms roughnesses for preprocessed samples are 5.1, 5.3, and 4.9 nm for the top, middle, and bottom samples, respectively. Postprocessed rms roughnesses for these samples are 2.9, 4.5, and 4.7 nm, respectively. Table II summarizes the rms roughness data. In this case, the surface roughness is also somewhat reduced after cleaning. Especially, the top sample which is closest to plasma source shows a significant reduction in roughness.

From the two sets of surface analysis results after cleaning, it appears that both plasma density and cleaning time affect Sn removal, oxidation, and surface roughness. The top sample was placed at the nearest position so it was exposed to a denser portion of the plasma, which is equivalent to more ion density. Since ions play an important role in increasing the number of active sites more and enhance surface reactions by hitting the surface, more cleaning is expected. This clearly shows that the removal rate of Sn is not uniform along the mock-up shells. Although Ru etches very slowly in this Ar/Cl₂ plasma, Ru can be susceptible to damages induced by plasma once the Sn is completely removed by plasma. Those damaged sites are more susceptible for oxidation even though Ru is used for the mirror surface because of its good oxidation resistance. To minimize the oxidation (the damage to the Ru) and maximize the cleaning with reliability, the plasma source location and cleaning time need to be carefully determined. The improved roughness can be explained by the fact that the cleaning removes Sn which ac-

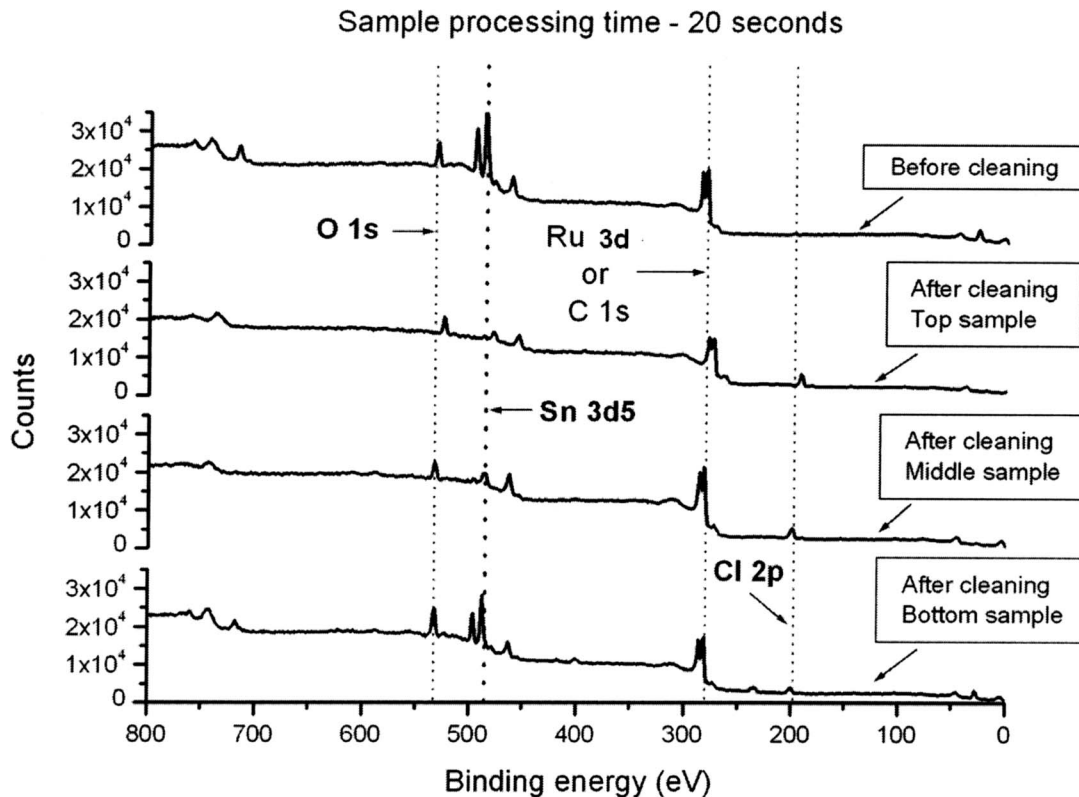


FIG. 11. XPS analysis of pre- and postprocessed samples. These are 3 nm of Sn deposited on Ru substrate in a real Sn EUV source. Cleaning was performed for 20 s. Sn peak can be seen very clearly on the sample before cleaning, whereas a considerable reduction in this peak is noticed after cleaning the Sn from samples at top and middle position on the mock-up shells. Bottom sample still shows the presence of Sn.

Sample processing time – 20 seconds

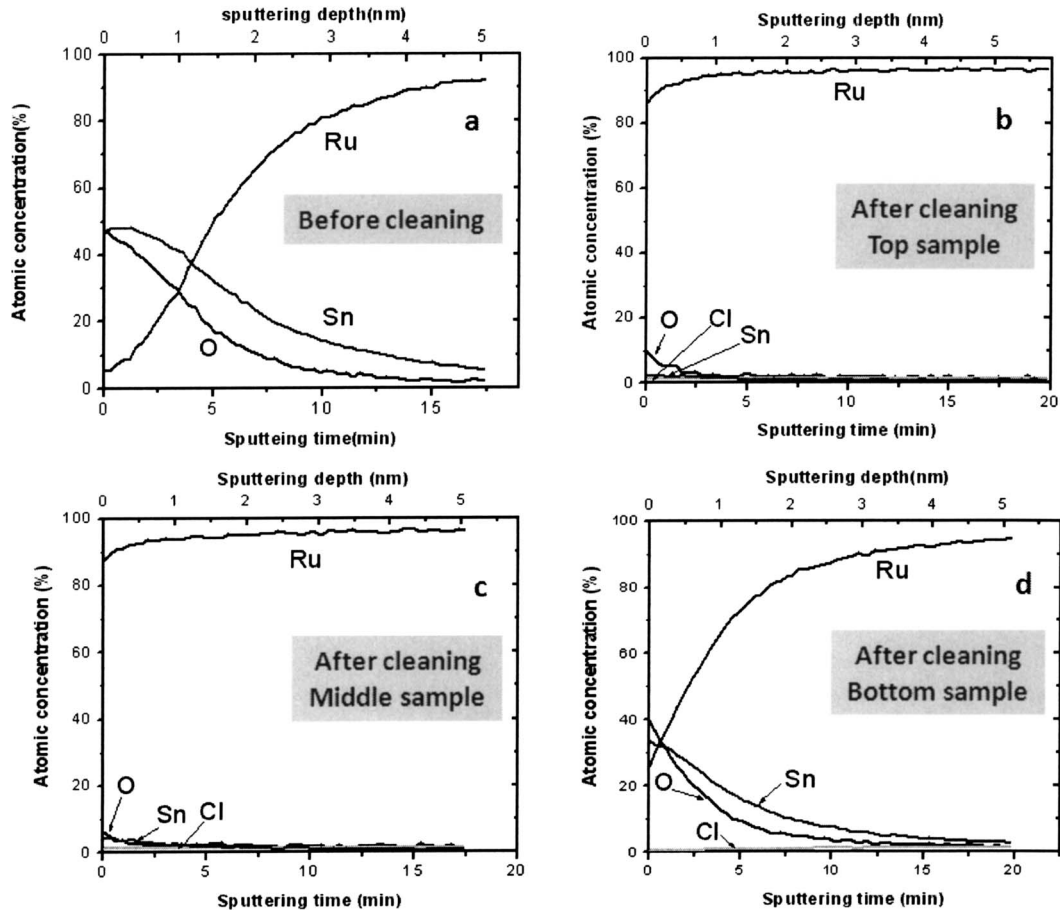


FIG. 12. AES analysis of pre- and postprocessed samples. These are 3 nm of Sn deposited on a Ru substrate in a real Sn EUV source. Cleaning was performed for 20 s. (a) Preprocessed sample, (b) postprocessed top sample, (c) postprocessed middle sample, and (d) postprocessed bottom sample. Sn is considerably removed from top and middle sample. Bottom sample still shows the presence of Sn.

Sample processing time – 20 seconds

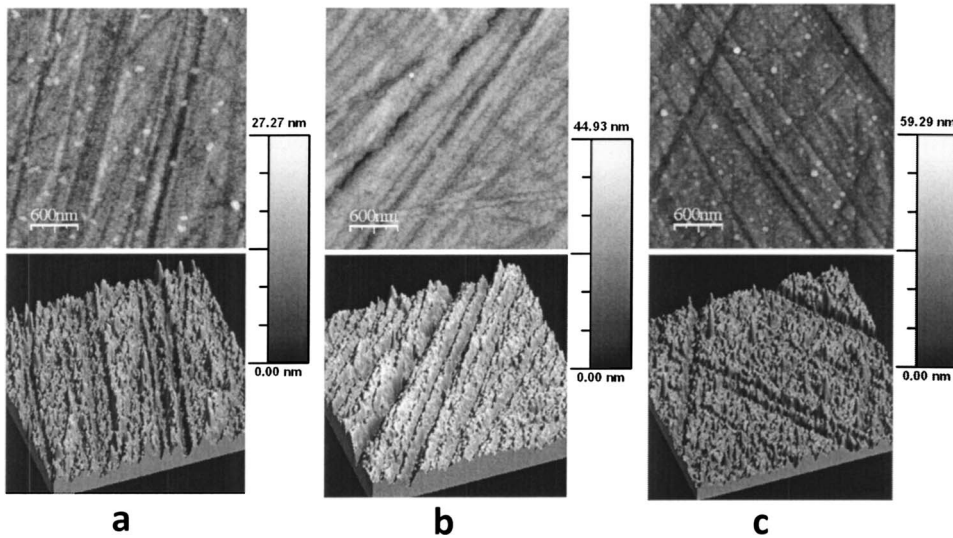


FIG. 13. AFM analysis of postprocessed samples. These are 3 nm of Sn deposited on a Ru substrate in a real Sn EUV source. Cleaning was performed for 20 s. (a) Postprocessed top sample, (b) postprocessed middle sample, and (c) postprocessed bottom sample.

TABLE II. AFM results of before-cleaning and after-cleaning samples after 20 s of processing time. The root mean square roughness (R_{rms}) and the maximum height (H_{max}) values for three postprocessed samples are shown in the table.

Position	Before cleaning		After cleaning	
	R_{rms}	H_{max}	R_{rms}	H_{max}
Top	5.1	59.6	2.9	30.5
Middle	5.3	70.4	4.5	67.1
Bottom	4.9	59.8	4.7	61.5

counts for the roughness of the samples before cleaning and reveals the smooth Ru surface underneath the Sn.

Results presented in this article are encouraging and can be developed for HVM needs. Whereas cleaning for only 20 s can still leave some Sn residue at the back of the collector mirrors, it was observed that 1 min of cleaning is very effective. Fortunately, portions of the mirror further from the source (and from the potential ICP coil location) will receive less Sn deposition in the first place. To integrate this technology in HVM, collector optics suppliers should optimize the parameters for their particular needs based on the plasma distribution and cleaning behavior. The technique could then be tested for various processing times, and compromise must be made depending on Sn removal, processing time, and mirror reflectivity. In this study, only the surface was investigated to see the feasibility of Sn cleaning with ICP-RIE. However, the reflectivity recovery after cleaning and more rigorous study of ICP source design should be followed in a further study before integrating this cleaning technique into the EUV source system.

IV. CONCLUSION

This article reports experimental works on the challenging problem in EUV lithography of finding a feasible and reliable solution to clean Sn from mirror surfaces. An inductively coupled plasma etching method was adopted to carry out the research using Ar/ Cl_2 gas mixtures. Sn etching was investigated for a variety of different experimental conditions, and the optimized etching results using different gas mixtures and sample biasing were presented. Also, water vapor pressure effect on Sn etching was presented. The Sn etch rate was found to be most dominantly affected by chuck bias. The Sn etch rate increases with higher bias, whereas the Ru or SiO_2 etch rate remains almost the same. This implies that the selectivity can be increased by increasing bias, but care must be taken as not to physically sputter off Ru or SiO_2 . A collector mock-up was constructed, and etching was performed on Sn coated samples placed at different locations on the collector shells. The results show that etch rates are di-

rectly dependent on plasma density and mirror geometry. Cleaning Sn from the Ru surface was performed, and the postprocessed sample surfaces were analyzed by XPS, AES, and AFM. The results show that all the Sn has been removed and that the Ru layer has no implantation damage from the cleaning cycle. However, under some conditions, the Ru surface was found to be oxidized, possibly caused by plasma damage. This work is the first step to integrate a cleaning system into a Sn EUV source. This work presents the feasibility of using an inductively coupled plasma etching as a method to clean Sn. For further steps, experiments using a real size cleaning system and more rigorous modeling studies are necessary. Reflectivity recovery test will also be necessary for the ultimate purpose of this study.

ACKNOWLEDGMENTS

The authors would like to thank USHIO for financially supporting this project. They would also like to thank Robert Bristol and Brian Jurczyk for their invaluable suggestions during the development phase of this project. They also thank the Center for Microanalysis of Materials, University of Illinois, which is partially supported by the U.S. Department of Energy under Grant No. DEFG02-91-ER45439. They also thank their undergraduate student Thomas Martino for his help and hard work on this project.

- ¹H. J. Levinson, *Principles of Lithography*, 2nd ed., SPIE Press Monograph Vol. PM146 (SPIE, Bellingham, WA, 2005), p. 19.
- ²I. V. Fomenkov *et al.*, *J. Phys. D* **37**, 3266 (2004).
- ³B. E. Jurczyk *et al.*, *Proc. SPIE* **5751**, 591 (2005).
- ⁴*CRC Handbook of Chemistry and Physics*, 66th ed. (CRC Press, Boca Raton, FL, 1985), p. B-153.
- ⁵V. Bakshi, *EUV Sources for Lithography*, edited by Vivek Bakshi (SPIE, Bellingham, WA, 2005), Chap. 1, p. 7.
- ⁶Y. Shimada *et al.*, *Appl. Phys. Lett.* **86**, 051501 (2005).
- ⁷D. N. Ruzic, *EUV Sources for Lithography*, edited by Vivek Bakshi (SPIE, Bellingham, WA, 2006), Chap. 36, p. 969.
- ⁸D. N. Ruzic, K. C. Thompson, B. E. Jurczyk, E. L. Antonsen, S. N. Srivastava, and J. B. Spencer, *IEEE Trans. Plasma Sci.* **35-3**, 606 (2007).
- ⁹Y. Teramoto *et al.*, *Proc. SPIE* **6517**, 5173R-1 (2007).
- ¹⁰S. S. Harilal, M. S. Tillack, Y. Tao, and B. O'Shay, *Opt. Lett.* **31**, 1549 (2006).
- ¹¹S. Graham, C. Steinhaus, M. Clift, L. Klebanoff, and S. Bajt, *Proc. SPIE* **5037**, 460 (2003).
- ¹²D. J. W. Klunder, M. M. J. W. v. Herpen, V. Y. Banine, and K. Gielissen, *Proc. SPIE* **5751**, 943 (2005).
- ¹³S. Bajt *et al.*, *Appl. Opt.* **42-28**, 5750 (2003).
- ¹⁴K. Okimura and J. Oyanagi, *J. Vac. Sci. Technol. A* **22**, p. 39 (2004).
- ¹⁵D. N. Ruzic, *Electric Probes for Low Temperature Plasmas* (AVS, New York, 1994), p. 51.
- ¹⁶K. J. Laidler, *Catalysis* (Reinhold, New York, 1954), Vol. 1, p. 128.
- ¹⁷R. d'Agostino, P. Capezzuto, F. Cramarossa, and F. Fracassi, *Plasma Chem. Plasma Process.* **9**, 513 (1989).
- ¹⁸D. M. Manos and D. L. Flamm, *Plasma Etching: An Introduction* (Academic, New York, 1989), p. 32.
- ¹⁹B. L. Henke, E. M. Gullikson, and J. C. Davis, *At. Data Nucl. Data Tables* **54**, 181 (1993).